

1
2
3
4
5
6
7
8
9
10
11
12
13

SUPPLEMENTAL INFORMATION:

How can mountaintop CO₂ observations be used to constrain regional carbon fluxes?

John C. Lin¹, Derek V. Mallia¹, Dien Wu¹, Britton B. Stephens²

¹Department of Atmospheric Sciences, University of Utah, Salt Lake City, Utah 84112, USA

²Earth Observing Laboratory, National Center for Atmospheric Research, Boulder, Colorado 80301, USA

Correspondence to: John C. Lin (John.Lin@utah.edu)

Manuscript Submitted to Atmospheric Chemistry and Physics

Fig. S1

Three-dimensional plots of the terrain over a domain of $\sim 1^\circ \times 1^\circ$ surrounding the NWR site, as resolved by the WRF 1.3-km model. The NWR site is indicated by the triangle. A small subsample of the numerous stochastic trajectories simulated by STILT, driven by WRF started at 2100 UTC (1400 MST), are drawn as black lines. Also shown is the average back trajectory (pink), derived by averaging locations of the stochastic trajectories. In addition, the PBL heights averaged along the backtrajectory are shown as the blue line.

22
23

24 **Adjusting the CT-2013b diurnal cycle**

25 In the CarbonTracker assimilation process, attempts to match CO₂ observations could
26 result in “dipoles” in scaling factors between nearby ecoregions, leading to negative
27 fluxes even at night (Fig. S2a). While respiration can occur during the day when
28 vegetation is under stress (e.g., droughts), photosynthetic uptake (negative fluxes) at
29 night, in the absence of sunlight, is biologically unphysical. In order to correct the
30 reversed diurnal cycle seen in CarbonTracker, a reversal had to be first detected within
31 CarbonTracker for the selected grid cell for a given day. Once the reversal was detected,
32 the sign of the biospheric flux was flipped. The positive flux was then adjusted so that the
33 net flux for the selected gridcell for the given day was equal to 0. Finally, the negative
34 flux was adjusted so that the final net flux was equal to the original net flux, which
35 preserved the total net flux for the day (Fig. S3). The resulting biospheric flux pattern can
36 seen in Fig. S2b.

37

38 **Fig. S2**

39 Mean biospheric fluxes from Jun~Aug 2012 averaged between 0600~0900 UTC
40 (2300~0200 MST). (a) Biospheric fluxes for the unmodified CarbonTracker flux fields
41 and (b) biospheric fluxes for the adjusted CarbonTracker flux fields. The black circle
42 represents HDP, the black diamond represents SPL, and the black star represents NWR.

43

44 **Fig. S3**

45 Schematic showing the adjustment of erroneous diurnal pattern in biospheric flux within
46 CarbonTracker (red line), with nighttime uptake, to a corrected biospheric flux (green
47 line). The dashed line represents a flux of 0.

48

49

50 **Fig. S4**

51 Average contributions to CO₂ variations at HDP, SPL, and NWR from biospheric,
52 anthropogenic, and wildfire fluxes at different times of the day between Jun~Aug 2012 as
53 simulated by STILT, driven with WRF-1.3km winds. Also shown are the observed
54 variations, calculated by subtracting out the STILT-derived background (see Sect. 2.3).

55

56 **Fig. S5**

57 Mean CO₂ concentrations extracted from the bottom 8 levels of CarbonTracker, in the
58 respective gridcells where the HDP, SPL, and NWR sites are located. The mean model
59 heights of the bottom 8 levels are (in meters AGL): 25, 103, 247, 480, 814, 1259, 1822,
60 2508. The concentrations interpolated to the heights of the 3 sites are indicated by the
61 orange dashed line. The observed values are drawn in black, with unfiltered data
62 (dashed) and after applying the filter for removing local influences (solid; Sect. 2.1).

63

64 **Fig. S6**

65 The average footprint (shown in log₁₀) for the SPL at 0200 MST (0900 UTC), gridded at
66 0.1°×0.1°. The site is denoted as a triangle. The average back trajectory (averaged over
67 the stochastic STILT trajectories) is drawn as a line, with points indicating trajectory
68 locations every hour, as the trajectory moves back from the site indicated as points. Red
69 parts of the trajectory refer to the nighttime (1900~0700 MST), while pink portions
70 indicate the daytime (0700~1900 MST). Parts of the trajectory are shaded with blue
71 when it is found below the average height of the PBL along the trajectory.

72

73 **Fig. S7**

74 Similar to Fig. S6, but for 1400 MST (2100 UTC).

75

76 **Fig. S8**

77 Similar to Fig. S6, but for the NWR site.

78

79 **Fig. S9**
80 Similar to Fig. S8, but for 1400 MST (2100 UTC).

81

82 **Fig. S10**
83 Three dimensional plots of the terrain over a domain of $\sim 1^\circ \times 1^\circ$ surrounding HDP, as
84 resolved by the WRF and GDAS models at various grid spacings. Also shown is the
85 average back trajectory, derived by averaging locations of the numerous stochastic
86 trajectories simulated by STILT, driven by the various WRF meteorological fields and
87 the global GDAS field. Back trajectories were started from HDP at 1400 MST (2100
88 UTC). Points indicate trajectory locations every hour, as the trajectory moves back from
89 the site indicated as points. Red portions of the trajectory refer to the nighttime
90 (1900~0700 MST), while pink portions indicate the daytime (0700~1900 MST). In
91 addition, the PBL heights averaged along the backtrajectory are shown as the blue line.

92

93 **Fig. S11**
94 Similar to Fig. S10, but for SPL.

95

96 **Fig. S12**
97 Similar to Fig. S10, but for NWR.

98

**2100 UTC
(1400 MST)**

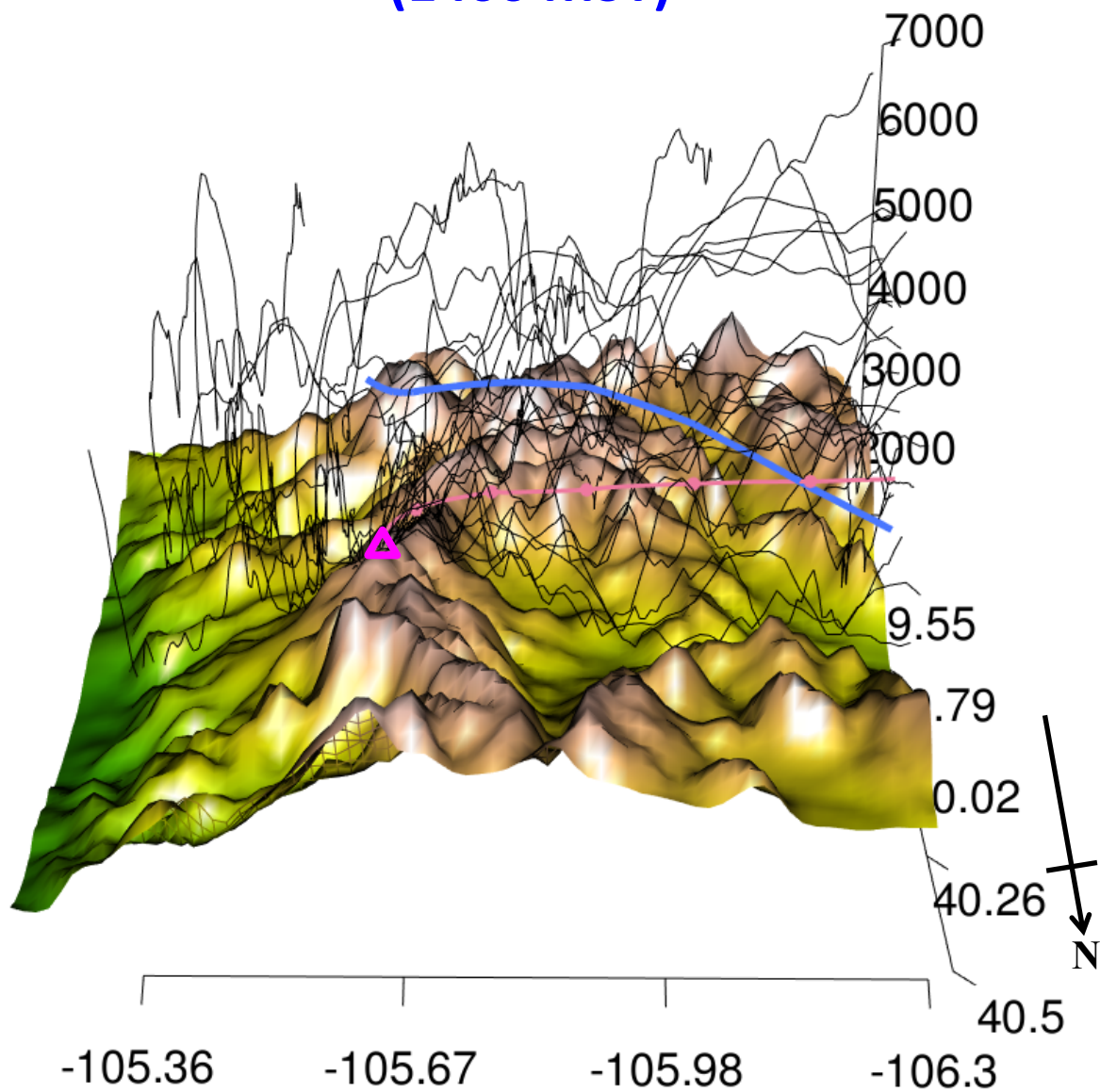


Fig. S1

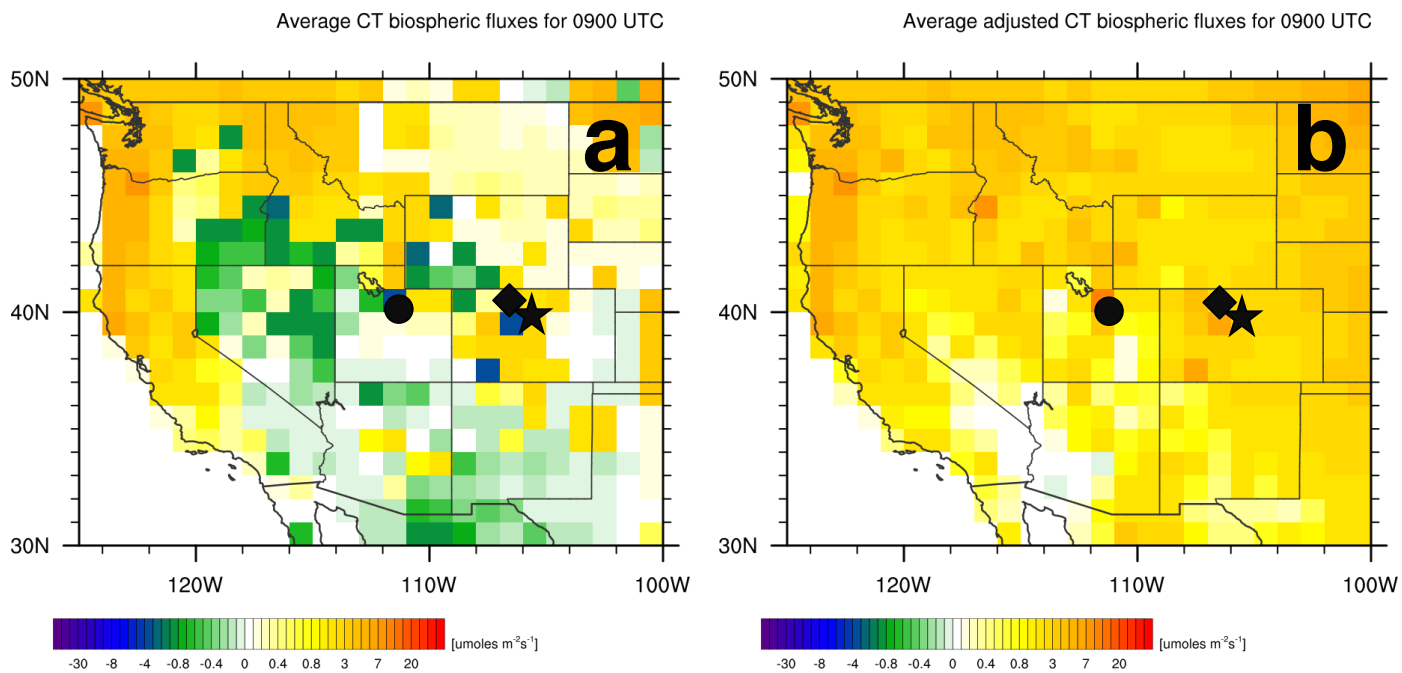


Fig. S2

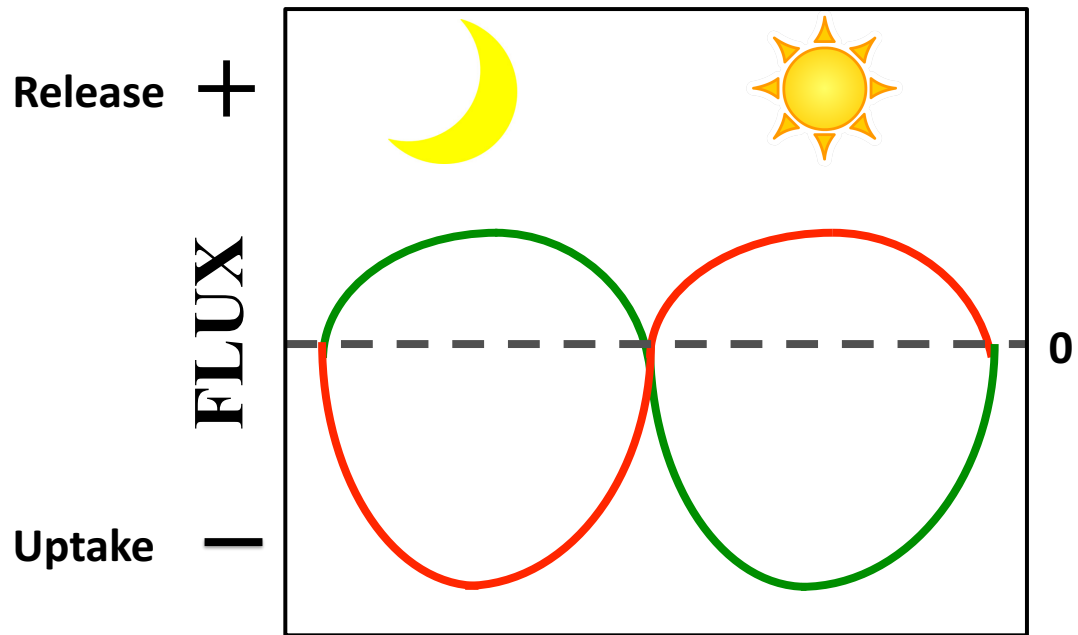


Fig. S3

Average Diurnal Contributions from Different CO₂ Sources

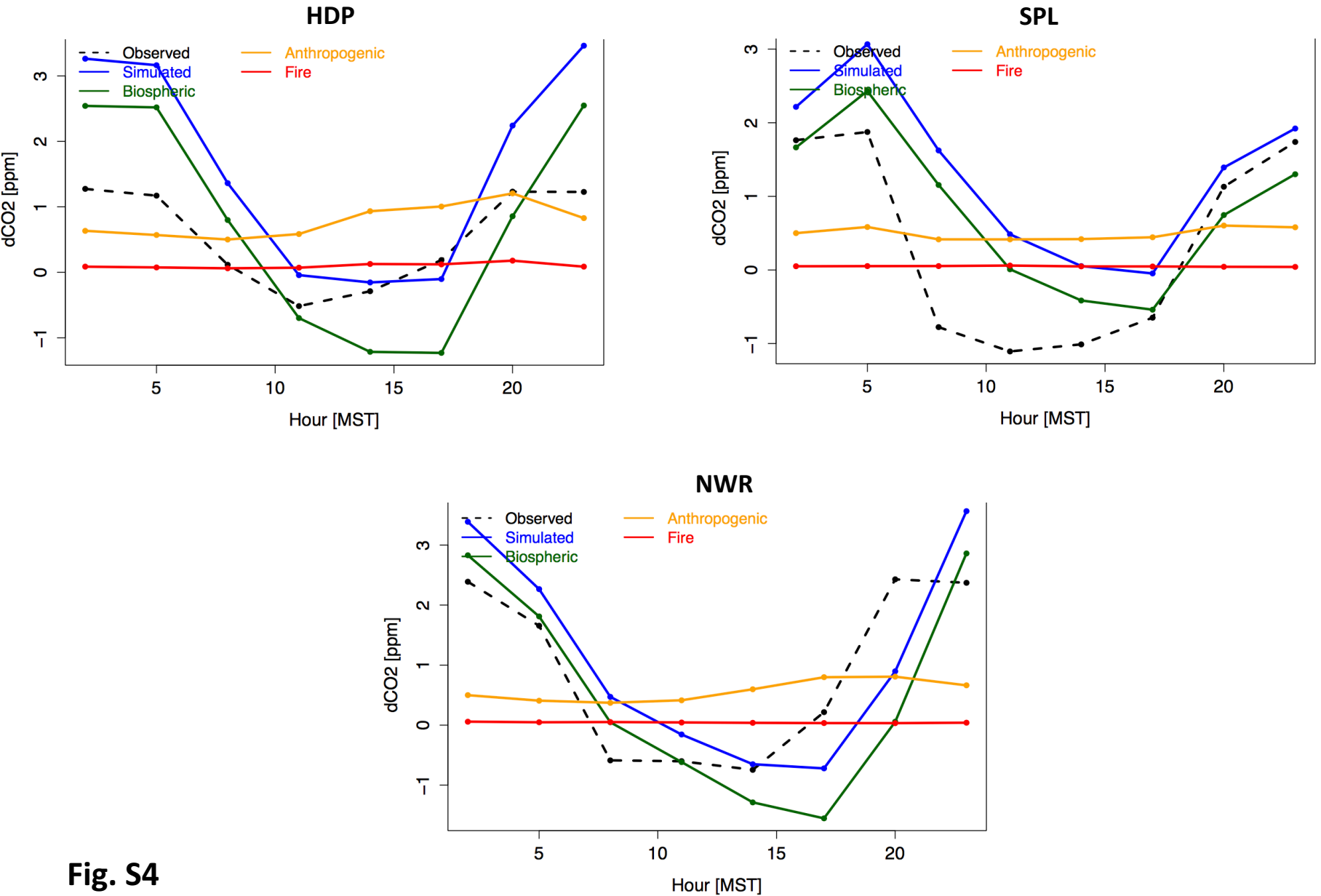
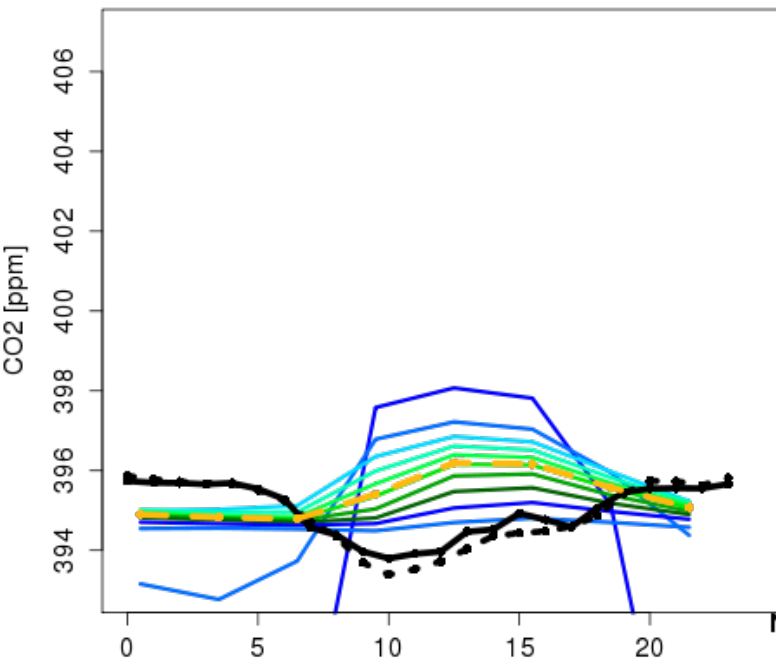
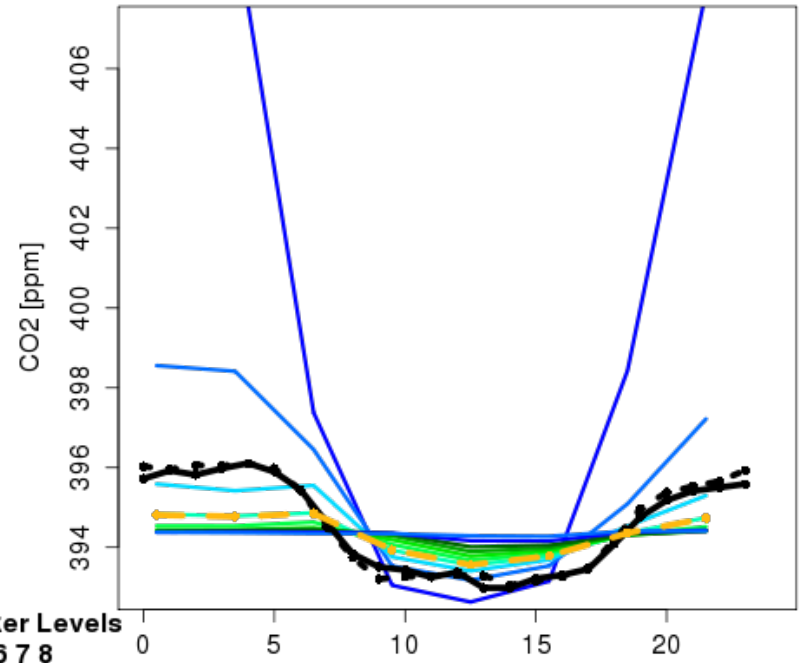


Fig. S4

HDP Carbon Tracker Levels
2012 MONs: 6 7 8

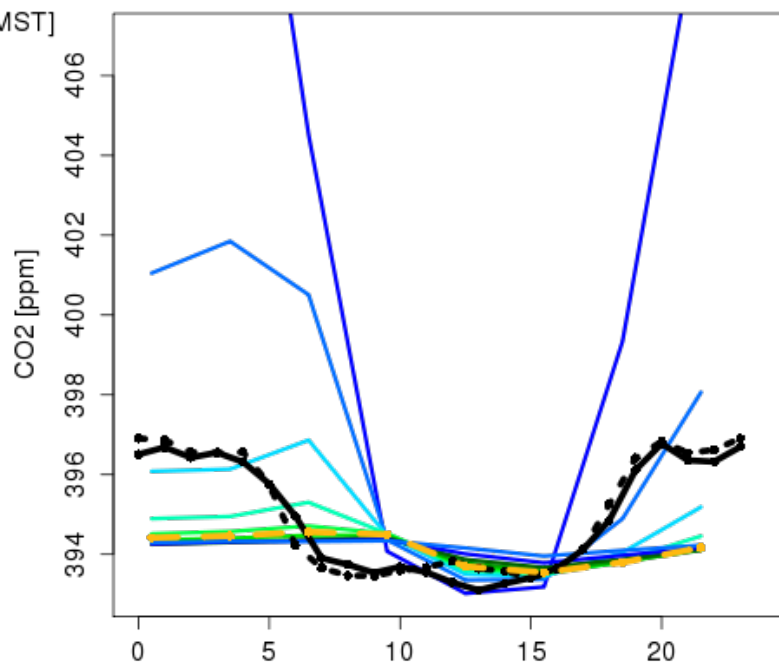


SPL Carbon Tracker Levels
2012 MONs: 6 7 8



NWR Carbon Tracker Levels
2012 MONs: 6 7 8

Time of Day [MST]



Time of Day [MST]

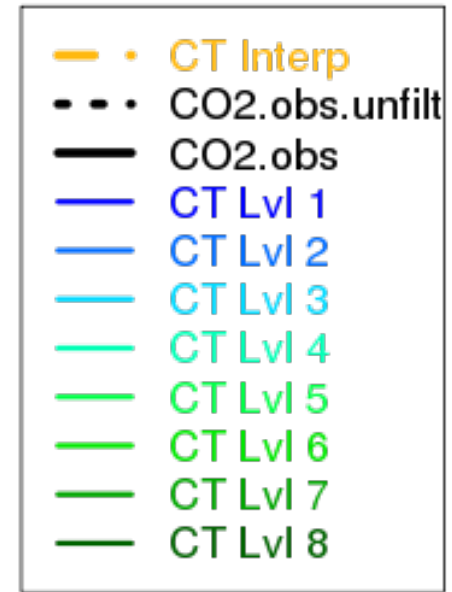
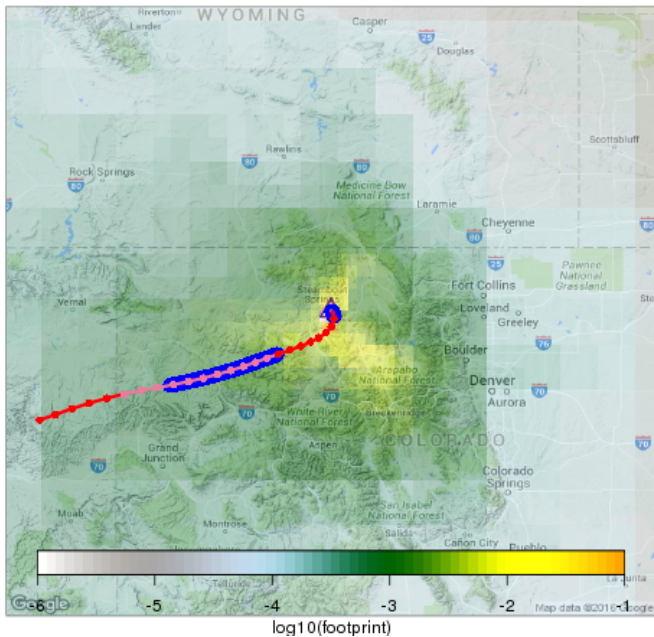
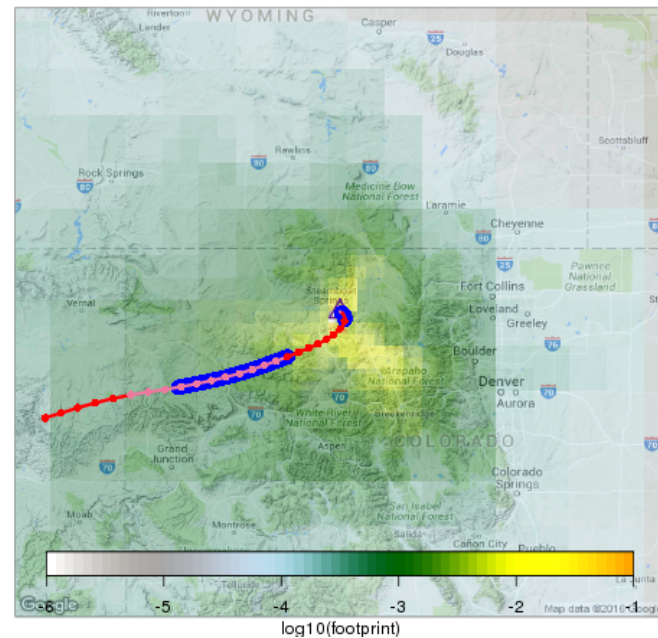


Fig. S5

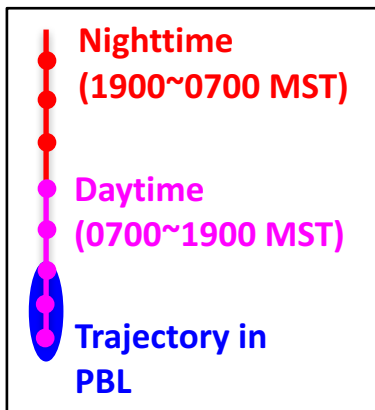
SPL ave footprint: WRF-1.3km (AGL)



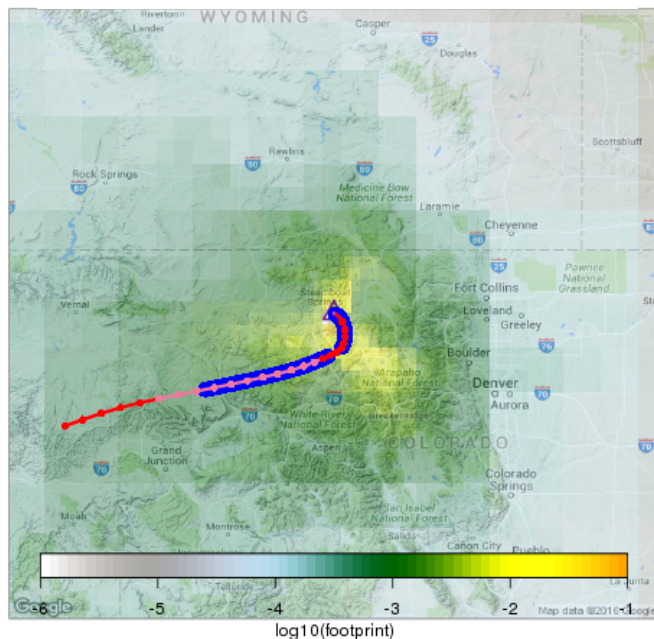
SPL ave footprint: WRF-4km (AGL)



0900 UTC
(0200 MST)



SPL ave footprint: WRF-12km (AGL)



SPL ave footprint: GDAS-1° (ASL)

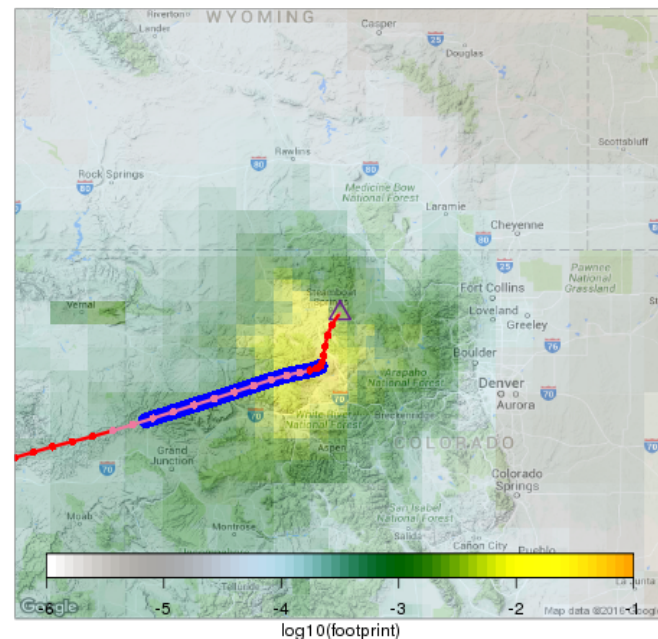
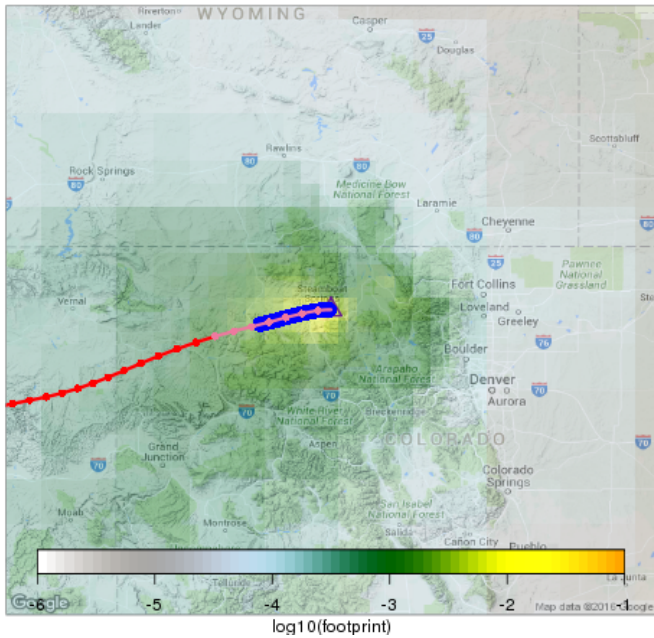
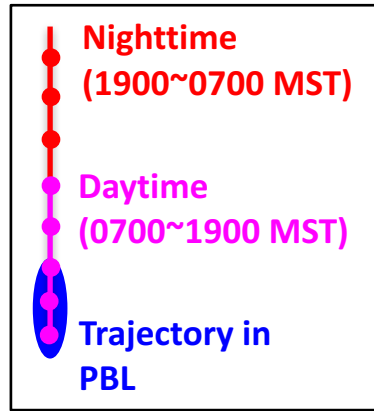


Fig. S6

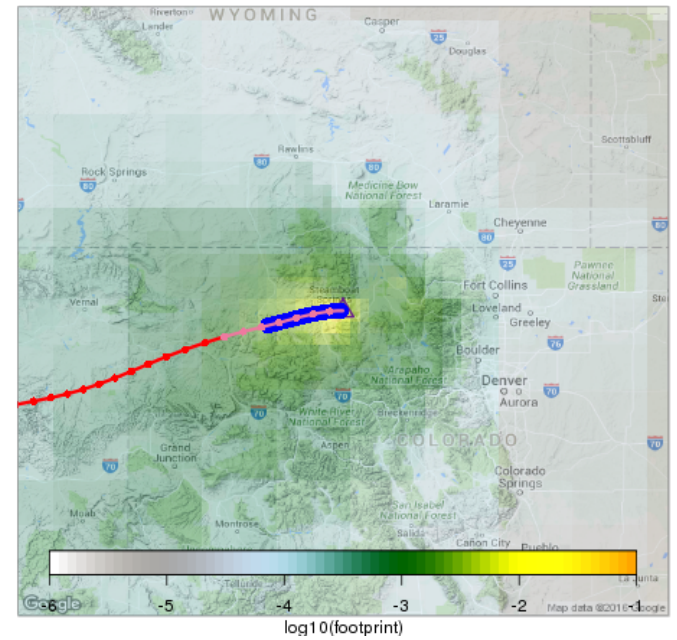
SPL ave footprint: WRF-1.3km (AGL)



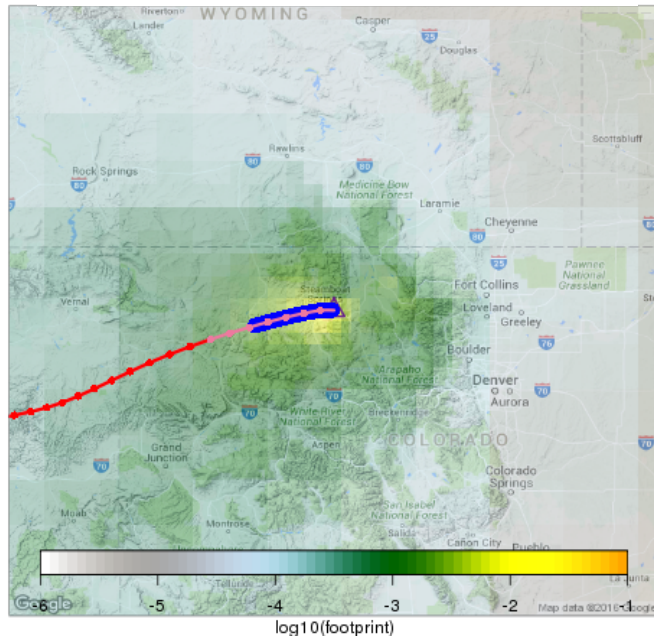
2100 UTC
(1400 MST)



SPL ave footprint: WRF-4km (AGL)



SPL ave footprint: WRF-12km (AGL)



SPL ave footprint: GDAS-1° (ASL)

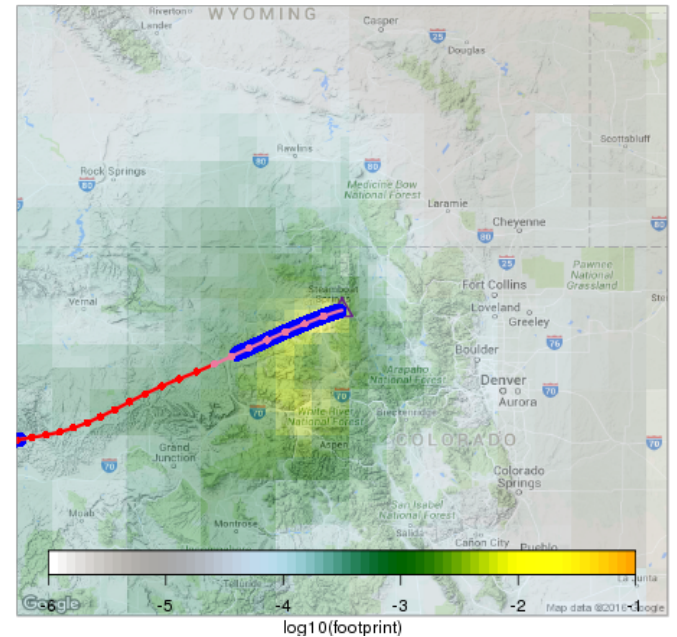
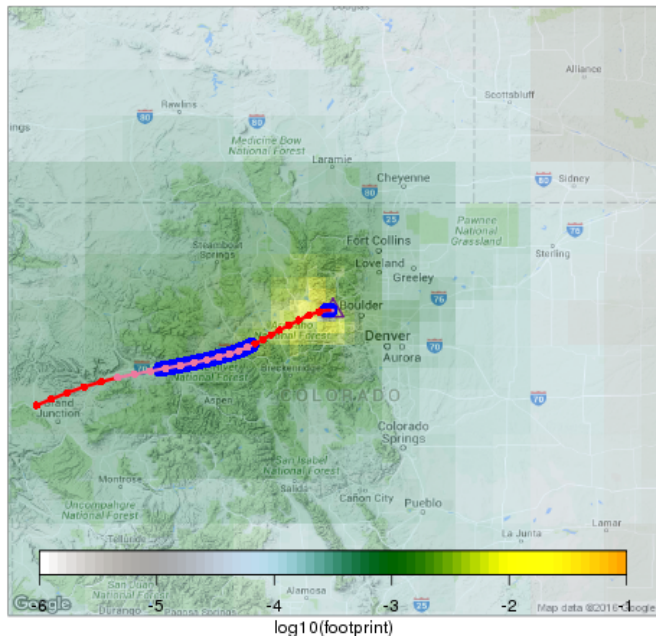
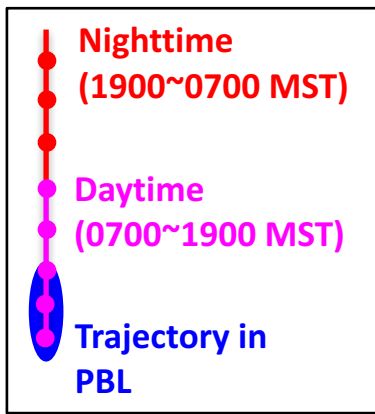


Fig. S7

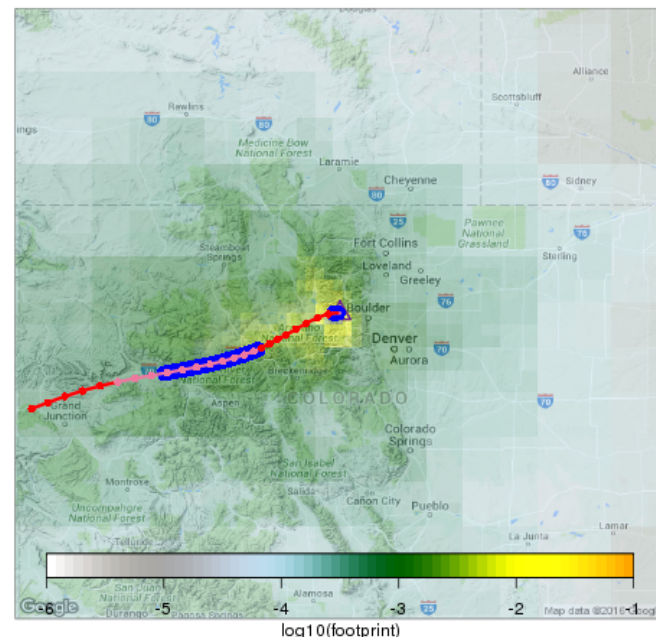
NWR ave footprint: WRF-1.3km (AGL)



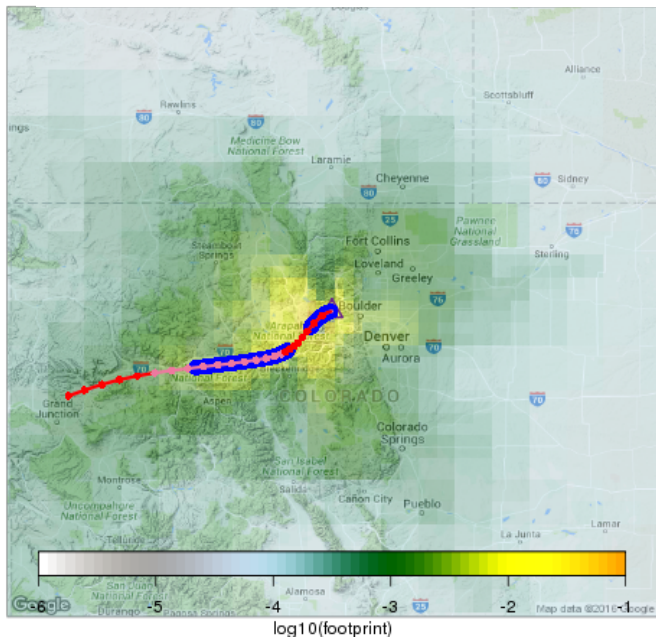
0900 UTC
(0200 MST)



NWR ave footprint: WRF-4km (AGL)



NWR ave footprint: WRF-12km (AGL)



NWR ave footprint: GDAS-1° (ASL)

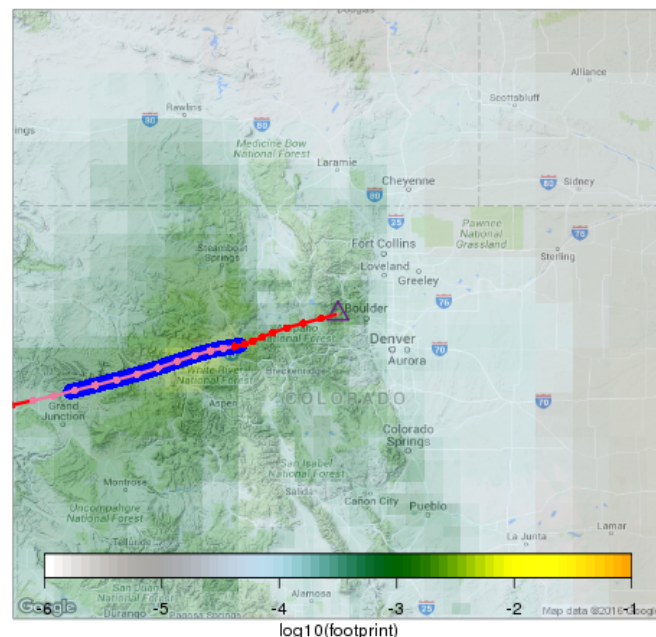
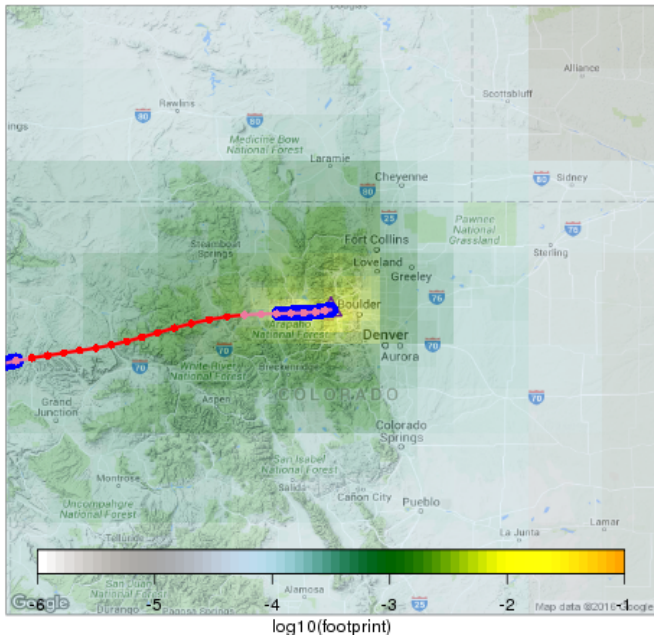
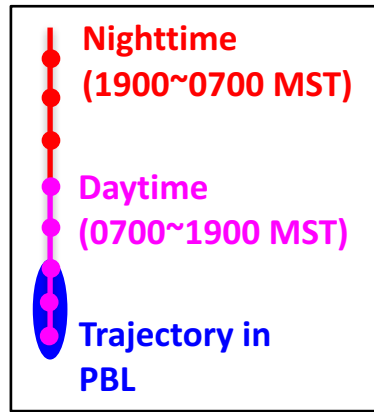


Fig. S8

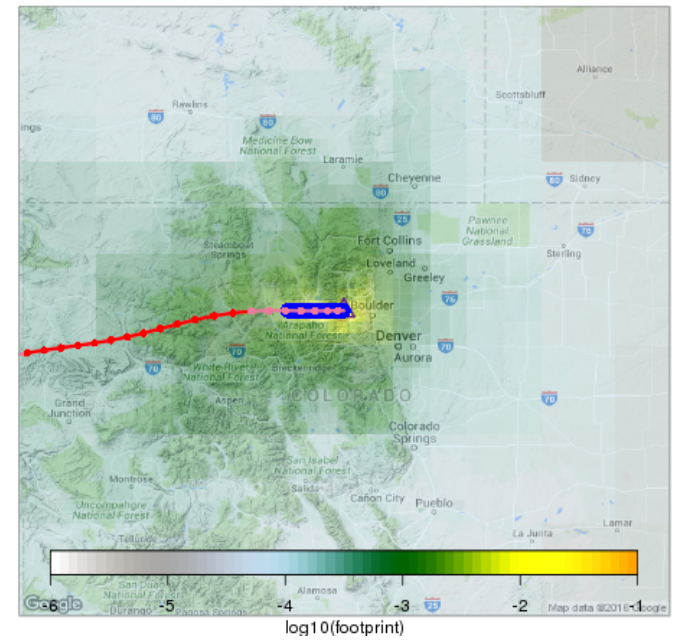
NWR ave footprint: WRF-1.3km (AGL)



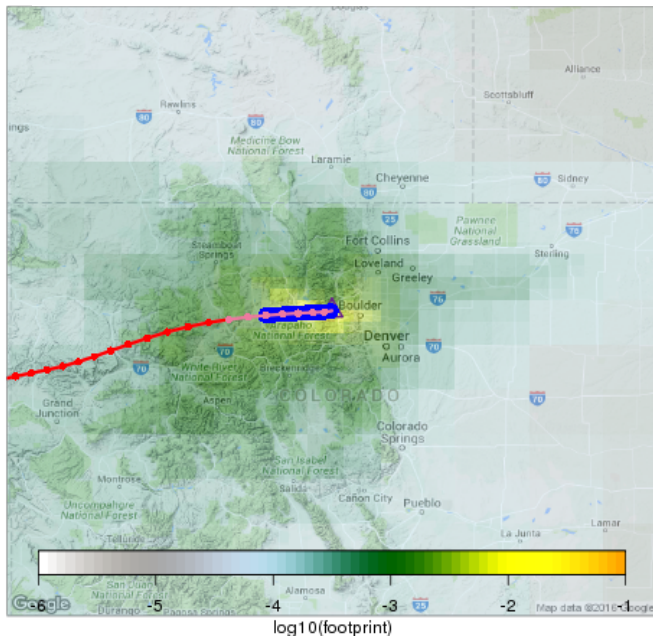
2100 UTC
(1400 MST)



NWR ave footprint: WRF-4km (AGL)



NWR ave footprint: WRF-12km (AGL)



NWR ave footprint: GDAS-1° (ASL)

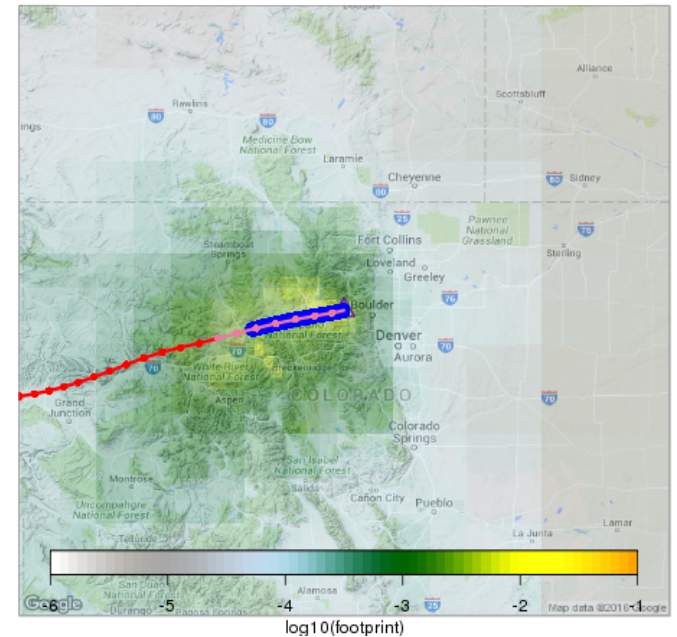


Fig. S9

HDP: Mean 3D Trajectory of Stochastic Particles & PBL ht for Different Runs

2100 UTC (1400 MST)

WRF-1.3km (AGL)

WRF-4km (AGL)

WRF-12km (AGL)

GDAS-1° (ASL)

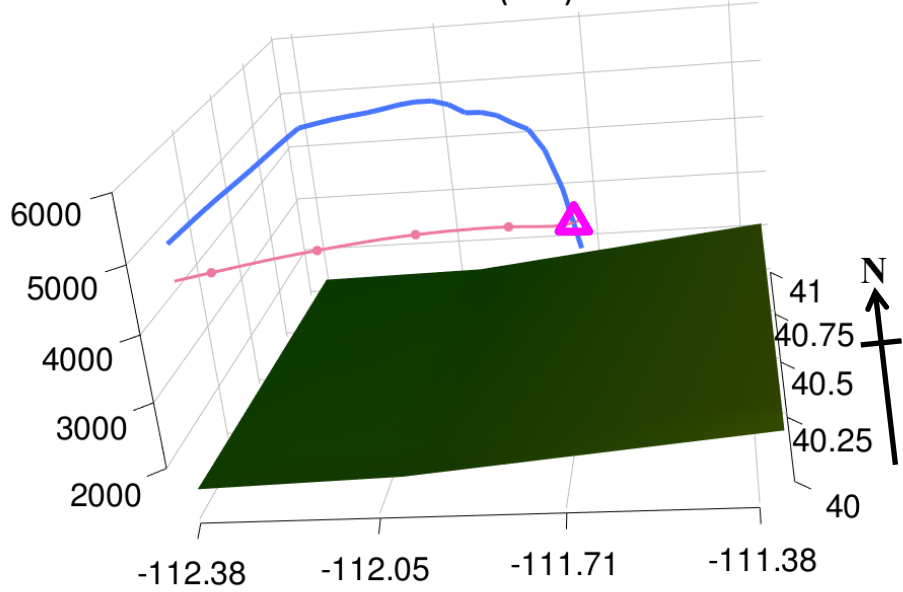
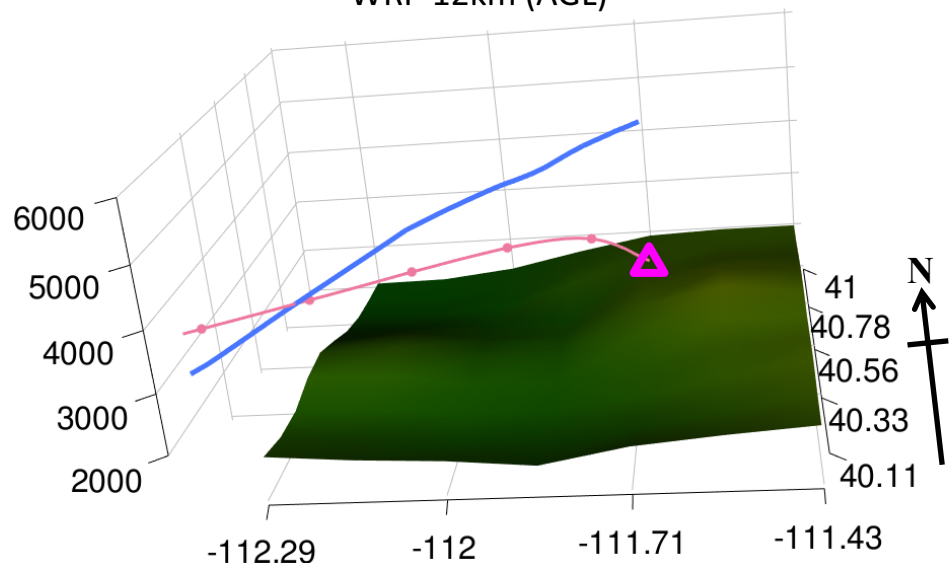
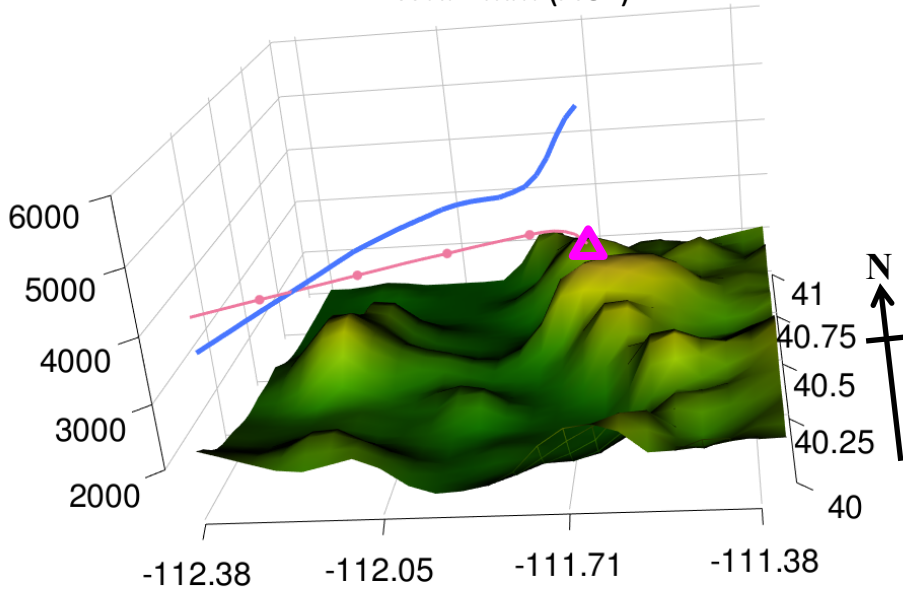
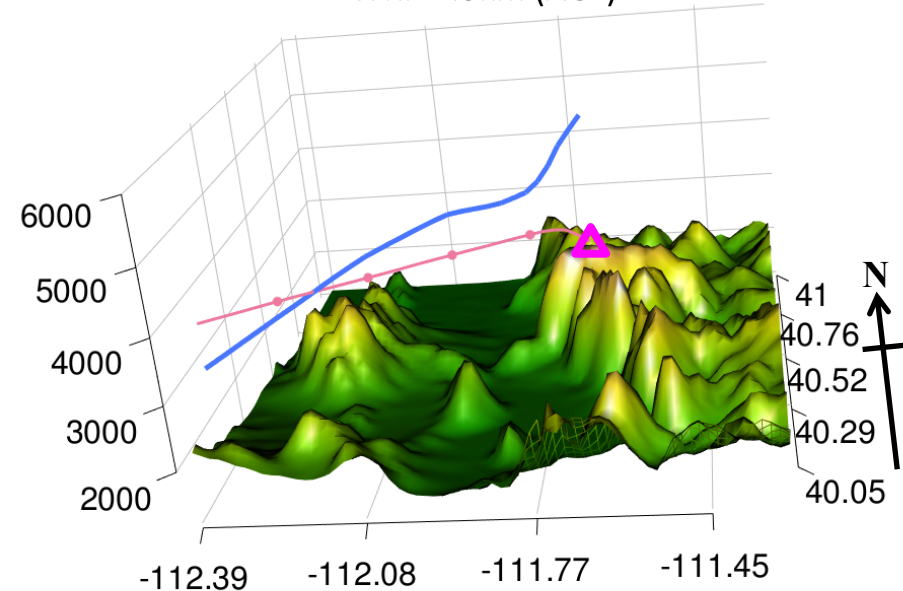
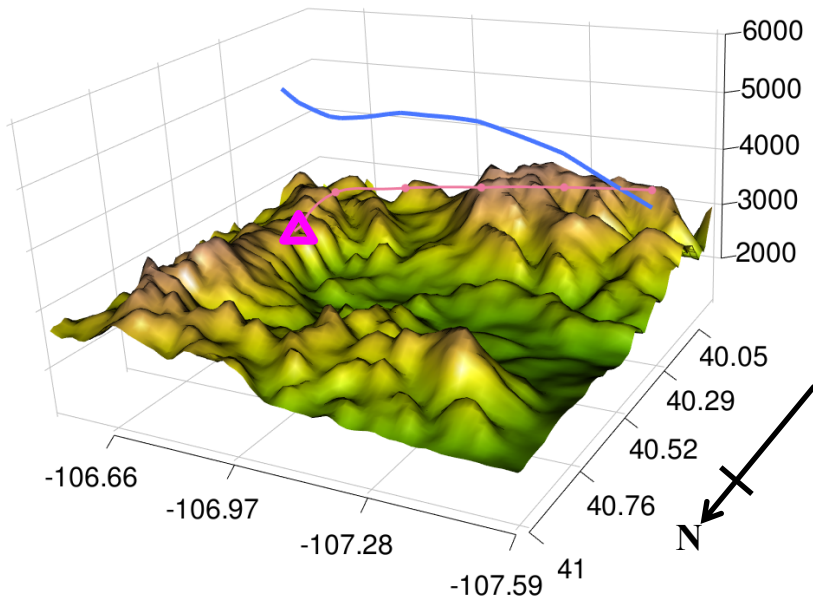


Fig. S10

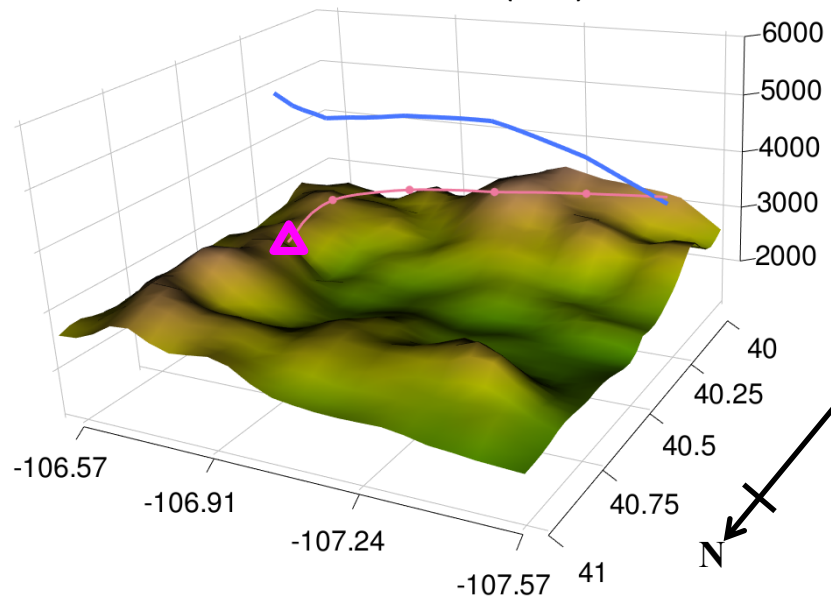
SPL: Mean 3D Trajectory of Stochastic Particles & PBL ht for Different Runs

2100 UTC (1400 MST)

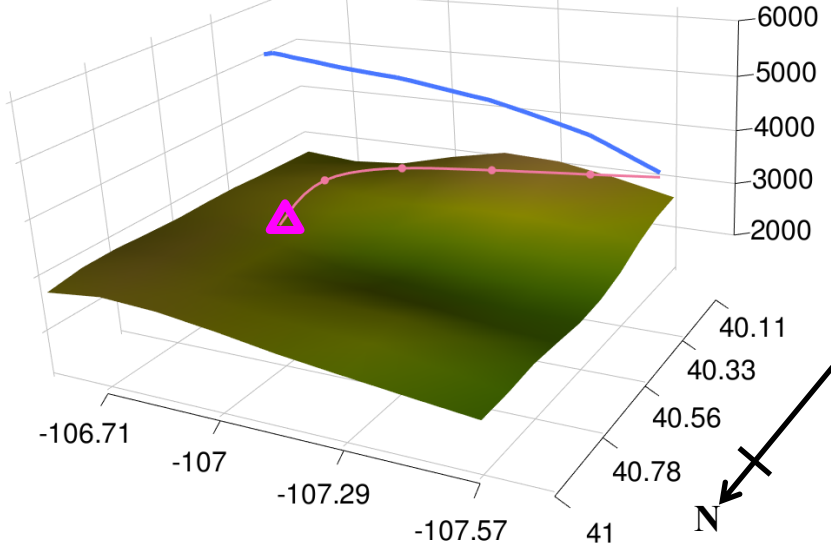
WRF-1.3km (AGL)



WRF-4km (AGL)



WRF-12km (AGL)



GDAS-1° (ASL)

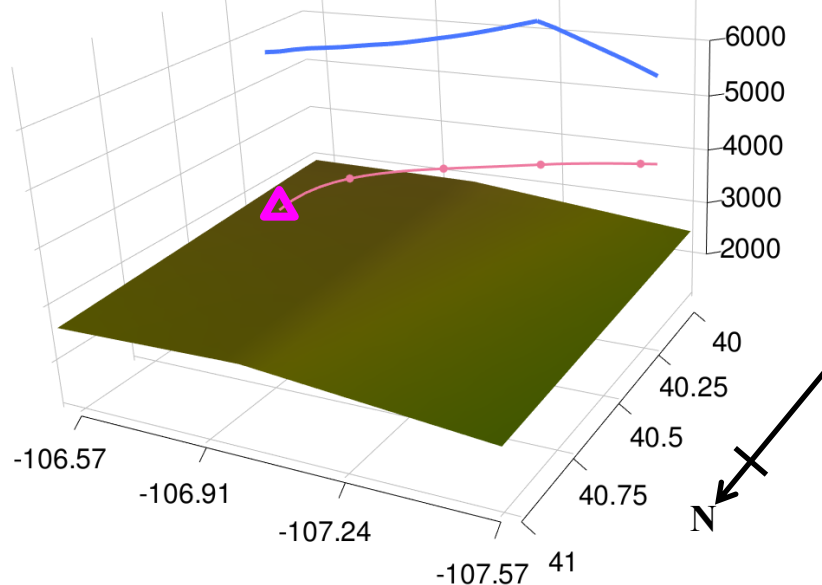


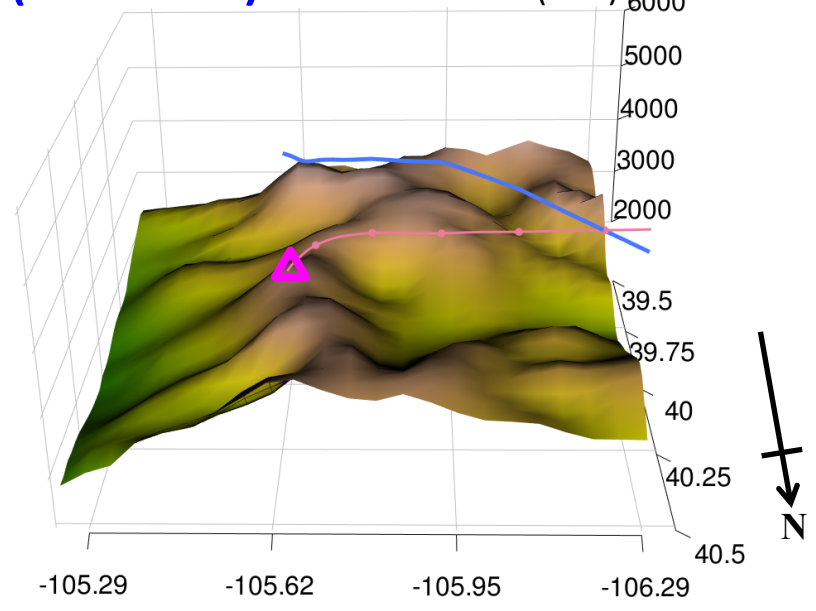
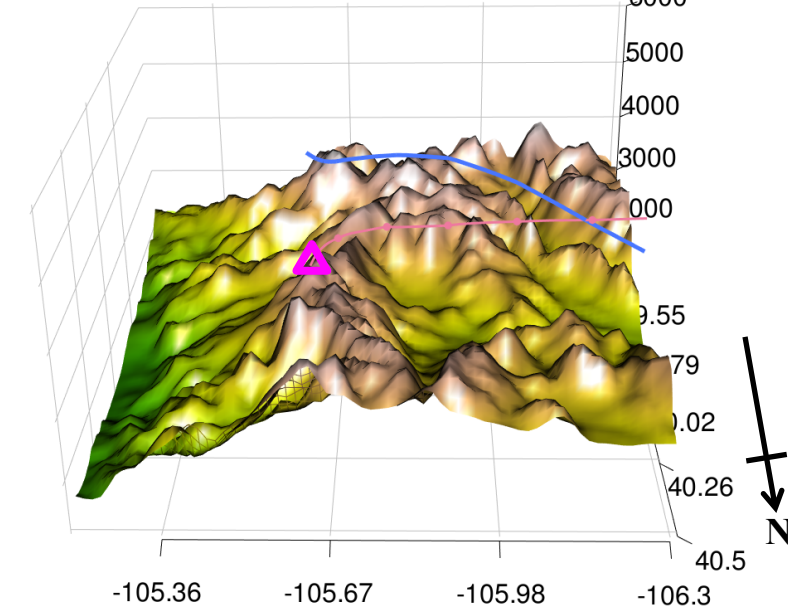
Fig. S11

NWR: Mean 3D Trajectory of Stochastic Particles & PBL ht for Different Runs

WRF-1.3km (AGL)

2100 UTC (1400 MST)

WRF-4km (AGL)



WRF-12km (AGL)

GDAS-1° (ASL)

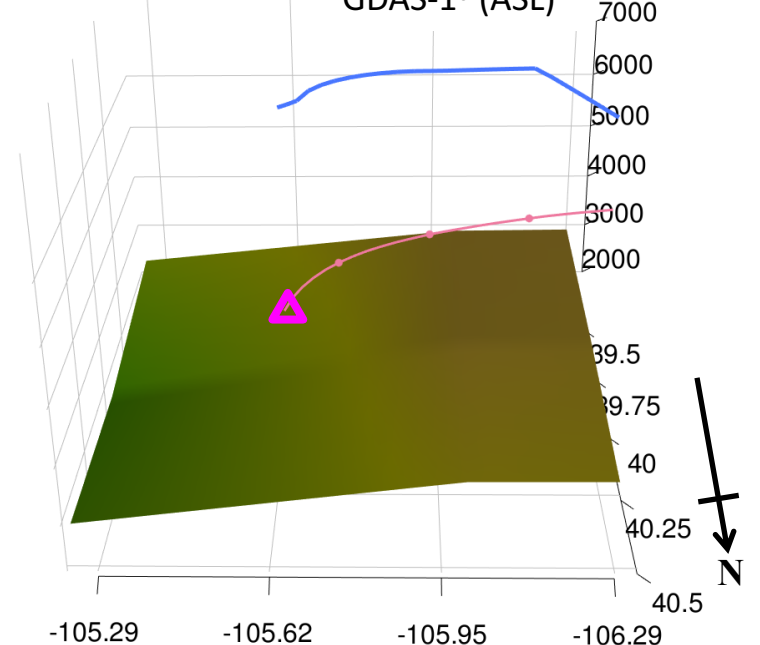
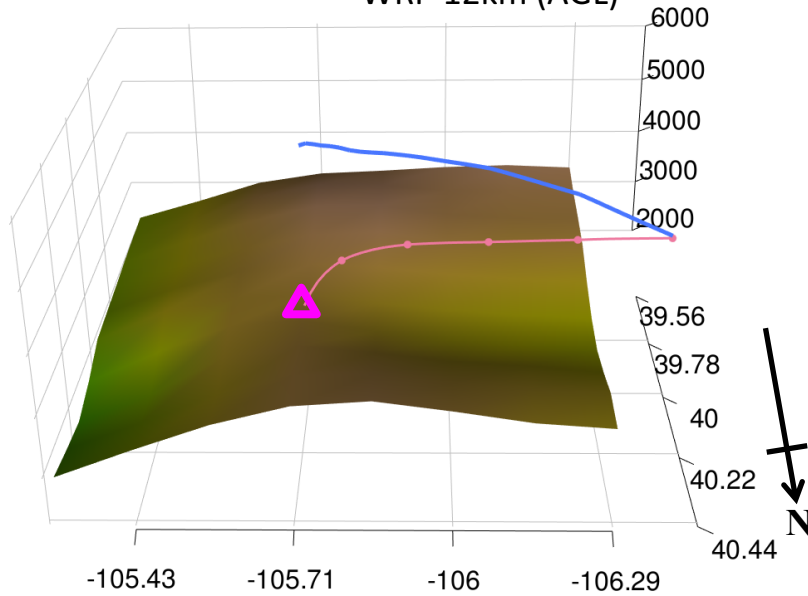


Fig. S12